Temporal evolution of the electric field accelerating electrons away from the auroral ionosphere

G. T. Marklund*, N. Ivchenko*, T. Karlsson*, A. Fazakerley†, M. Dunlop‡, P.-A. Lindqvist*, S. Buchert§, C. Owen†, M. Taylor†, A. Vaivalds§, P. Carter†, M. André§ & A. Balogh‡

** Division of Plasma Physics, Alfvén Laboratory, KTH, Royal Institute of Technology, SE 10044 Stockholm, Sweden*
† University College, London, Mullard Space Science Laboratory, Holmbury St Mary, Dorking, Surrey RH5 6NT, UK
‡ Imperial College, Blackett Laboratory, Space and Atmospheric Physics Group, London SW7 2BW, UK
§ Swedish Institute of Space Physics, Ångströmlaboratoriet, Box 534, SE 751 21 Uppsala, Sweden

The bright night-time aurorae that are visible to the unaided eye are caused by electrons accelerated towards Earth by an upward-pointing electric field[1–3]. On adjacent geomagnetic field lines the reverse process occurs: a downward-pointing electric field accelerates electrons away from Earth[4–11]. Such magnetic-field-aligned electric fields in the collisionless plasma above the auroral ionosphere have been predicted[12], but how they could be maintained is still a matter for debate[13]. The spatial and temporal behaviour of the electric fields—a knowledge of which is crucial to an understanding of their nature—cannot be resolved uniquely by single satellite measurements. Here we report on the first observations

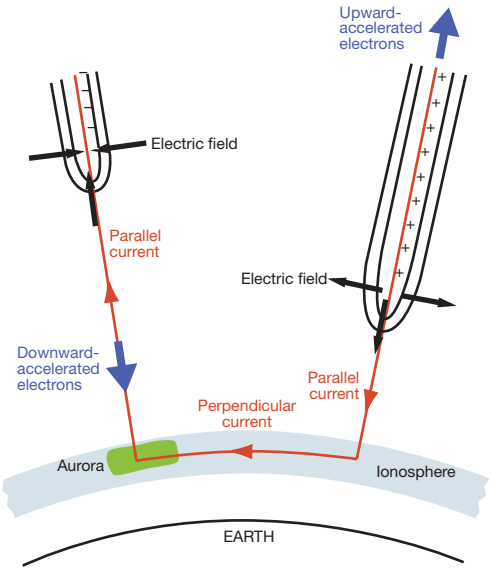

Figure 1 Acceleration structures (black) within the auroral current circuit (red). This diagram shows a negatively charged potential structure (indicated by equipotential contours) representative of the aurora (left) and a positively charged potential structure representative of the auroral return current (right). The two branches of the equipotential contours close at typical altitudes of 5,000–8,000 km in the upward-current region above the aurora and at 1,500–3,000 km in the auroral return-current region, respectively, above which they extend to very high altitudes along the geomagnetic field, forming the characteristic U-shape. The field-aligned currents are carried by the downward and upward accelerated electrons, respectively (blue). Together with the ionospheric closure current and the magnetospheric generator these form the complete auroral current circuit. The figure shows a north–south section through the structures that usually extend several hundreds of kilometres in the east–west direction.

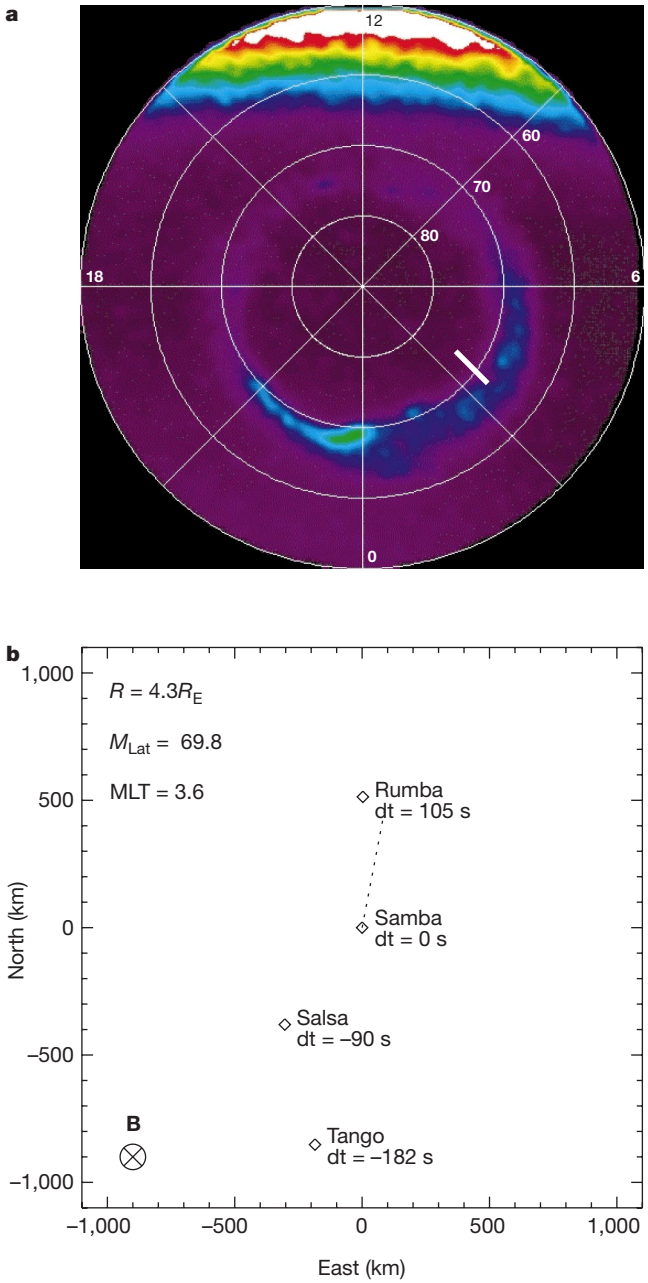

Figure 2 Location and configuration of the Cluster satellite formation passing over the Northern Hemisphere auroral oval. It passed between 4:20 and 4:40 UT on 14 January 2001, in the recovery phase of a weak substorm, peaking at 04:00 UT. **a**, The nightside auroral oval as observed by the ultraviolet imager on the IMAGE satellite at 04:30 UT. The post-midnight auroral oval forms a relatively homogeneous diffuse band between 65 and 70 degrees magnetic latitude. The ionospheric projection of the Cluster orbit (between 4:20 and 04:45 UT) is shown by the white line intersecting the auroral oval near 3:00 magnetic local time. **b**, Cluster satellite configuration on 14 January 2001. Relative positions and time differences (dt) between the Cluster 1, 2, and 4 spacecraft with respect to the reference Cluster spacecraft 3 (Samba) in a plane transverse to the magnetic field. The four Cluster spacecraft are aligned nearly as pearls on a string, with the separation transverse to the velocity vector being small, and follow in the sequence 1-3-2-4. The direction of motion of Samba projected onto this plane is shown by the dotted line. **B** denotes the direction of the geomagnetic field, R is the geocentric distance of the Samba spacecraft expressed in units of the Earth radius (R_E), M_{Lat} denotes magnetic latitude, and MTL denotes magnetic local time.

by a formation of identically instrumented satellites crossing a beam of upward-accelerated electrons. The structure of the electric potential accelerating the beam grew in magnitude and width for about 200 s, accompanied by a widening of the downward-current sheet, with the total current remaining constant. The 200-s timescale suggests that the evacuation of the electrons from the ionosphere contributes to the formation of the downward-pointing magnetic-field-aligned electric fields. This evolution implies a growing load in the downward leg of the current circuit, which may affect the visible discrete aurorae.

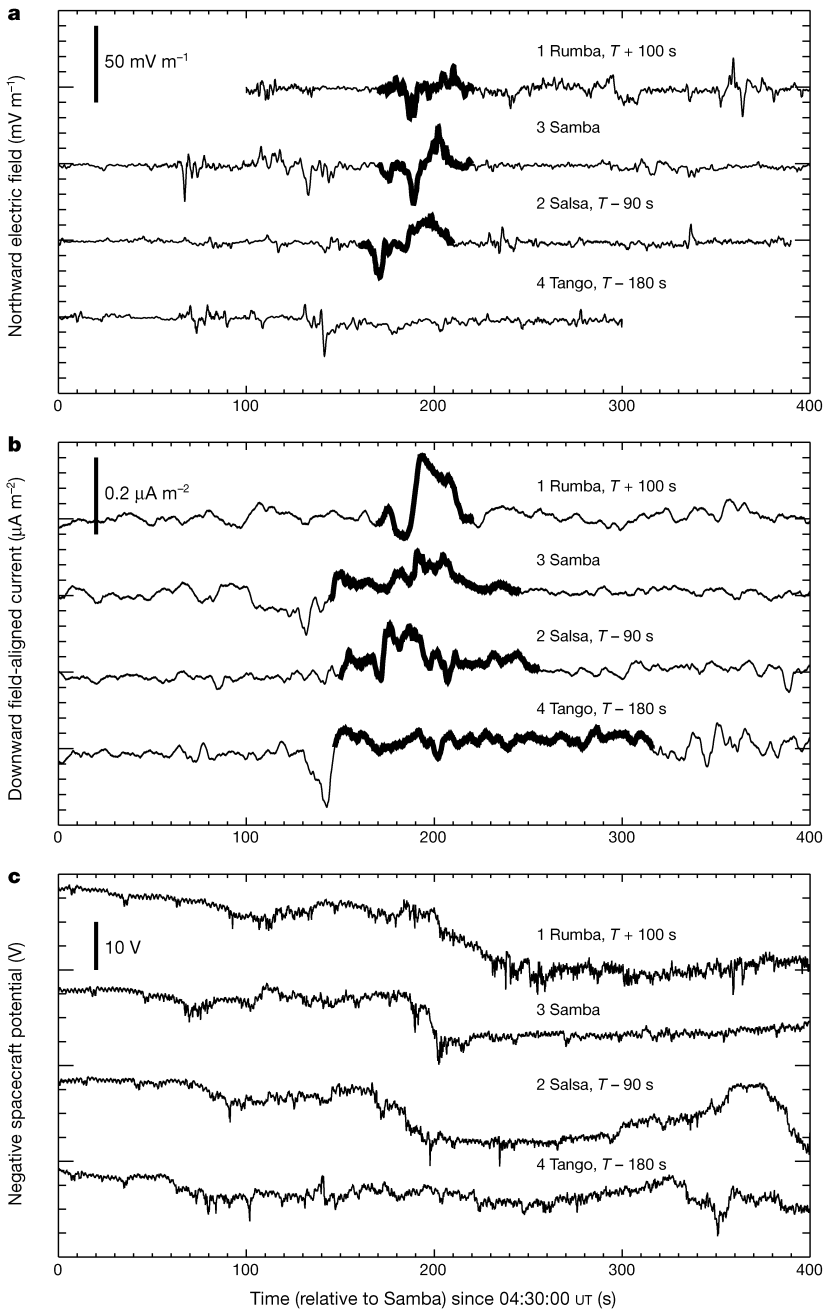

Figure 3 Evolution of the electric field, magnetic field-aligned current, and plasma density between the four crossings. The time axes for all satellites except for Samba (T) are shifted to account for the time delay between the satellites. **a**, Geomagnetically northward electric field component normal to the magnetic field, derived from measurements by the Electric Field and Wave (EFW) instrument onboard the four satellites. The bipolar structure (a southward excursion followed by a northward excursion) is highlighted in bold in the centre of each panel. It is seen to grow both in latitudinal width (from 15 km to 25 km projected to the ionospheric level) and magnitude between the first three crossings and then fade away by the time of the last crossing. Electric potentials obtained by integration along the orbit increase from 0.4 kV on Rumba, to 1.7 kV on Samba, to over 2 kV on Salsa. **b**, Field-aligned current derived from the geomagnetic east-west variation of the magnetic field, measured by the Flux Gate Magnetometer (FGM) instrument. A downward-current sheet is co-located with the bipolar structures. The total current integrated over the sheet is roughly constant, but the current density decreases between the consecutive crossings, as the current sheet widens. The most significant widening occurs between the last two crossings. **c**, Negative of the spacecraft potential, as measured by the EFW instrument. The spacecraft potential depends primarily on the ambient plasma density, and is thus a monitor thereof. The electric-field structure is co-located with a density gradient in the first three crossings, separating a region of higher and less variable densities southward of the structure from a region of low and variable densities to the north. At the time of the fourth crossing the density gradient is no longer seen.

In situ observations of electric fields, field-aligned currents, and energetic electrons and ions made by numerous satellites above and below the regions where the auroral acceleration takes place have been used to confirm[1–3] that the quasi-static electric potential structures formed above the aurora are typically U-shaped and negatively charged, as first suggested in ref. 14 on the basis of studies of the motion of auroral forms. These structures are aligned in the geomagnetic east–west direction, and are located in the region of upward-field-aligned current with an upward electric field (auroral acceleration region) at typical altitudes of 5,000–8,000 km (Fig. 1, left). A satellite moving poleward above the auroral acceleration region will measure the typical bipolar signature of a converging electric field and an upward beam of ions having a characteristic energy corresponding to the parallel potential drop below the satellite, whereas a satellite below this potential drop will observe accelerated auroral electrons and a much reduced electric field. The Swedish satellite Freja, with an apogee at 1,700 km, well below the lower limit of the auroral acceleration region, observed very intense (of the order of 1 V m^{-1}) and narrow (a few km) diverging electric fields[7,8] accompanied by upward fluxes of energetic electrons (a few keV)[9] on field lines adjacent to the aurora, where the downward current flows. These unexpected observations suggested that positively charged potential structures develop there (Fig. 1, right), forming the counterpart to the negative potential structures of the aurora. Now there is conclusive evidence, particularly from observations by the satellite FAST at higher altitudes around 4,000 km, to confirm this picture[10]. A few theories of how to maintain such a structure with a downward electric field have been suggested[4,6,15–17]. The Polar satellite, exploring the region at altitudes high above the acceleration region (19,000–38,000 km), has detected electric fields occasionally exceeding 100 mV m^{-1} (refs 18 and 19).

We need to understand the temporal behaviour of these structures to reveal by what mechanism they are formed. However, despite the excellent quality of the data from auroral missions such as Freja, FAST and Polar the spatio-temporal ambiguity inherent in these measurements prevented any conclusive answers. The European Space Agency mission Cluster[20,21], with four identically instrumented spacecraft (spacecraft 1, 2, 3 and 4 named Rumba, Salsa, Samba and Tango, respectively) in orbit since summer 2000, is the first ambitious and carefully planned attempt to carry out multipoint *in situ* measurements in the near-Earth space environment. Such measurements should be capable of solving this problem.

The Cluster observations presented here are from a poleward crossing of auroral field lines at an altitude of 22,000 km, where the

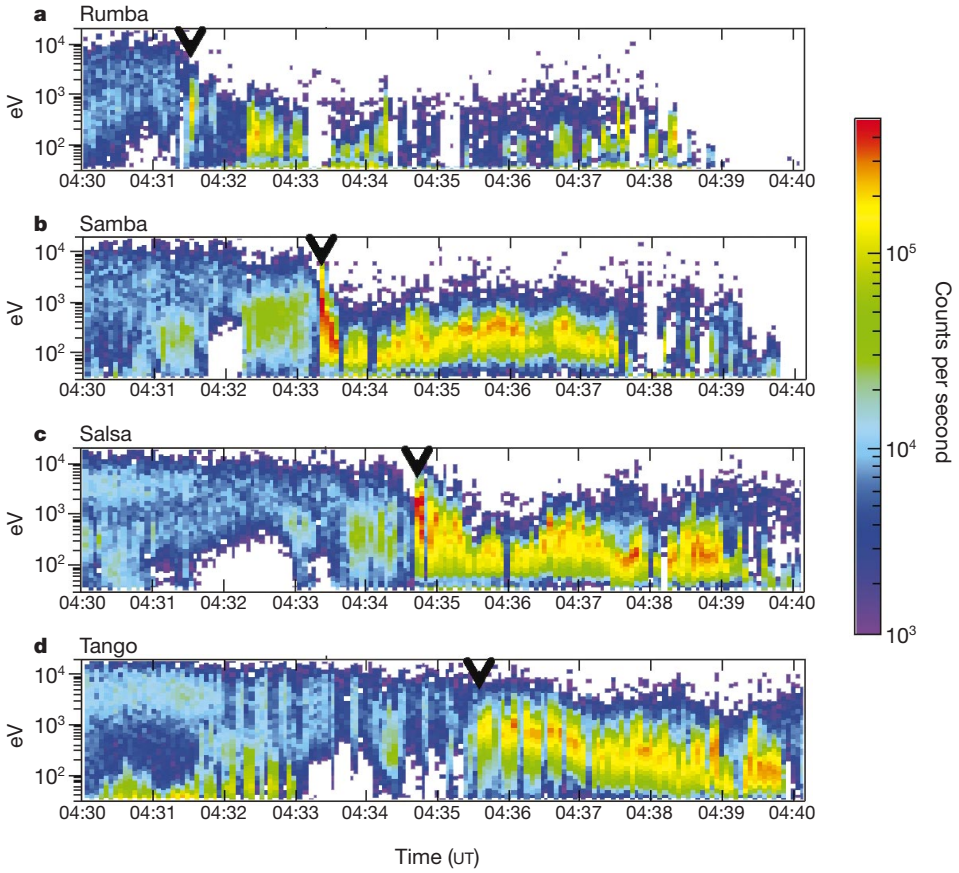

Figure 4 Upward-accelerated electron beam: evolution of energy and width. **a**–**d**, Time-energy spectrograms show electrons moving anti-parallel to the magnetic field as measured by the Plasma Electron and Current Experiment (PEACE) instrument between 4:30 and 4:40 UT, 14 January 2001 (the full pitch angle distribution is not shown here). The arrowheads at the top of the panels indicate the encounters with the bipolar-electric-field structures, occurring at a transition between two characteristically different electron populations, a high-energy isotropic electron population characteristic of the central plasma sheet to the south, and a lower-energy population characterized by intermittent, bi-directional, and field-aligned electron bursts, typical of the plasma sheet boundary layer to the north, and collocated with an upward more energetic electron beam. The beam (**b**) first increases in energy from about 0.7 keV on Rumba (**a**), to 1.2 keV on Samba (**b**), to 2 keV on Salsa (**c**), but at the time of the Tango crossing (**d**) the energy has dropped to 0.8 keV and the beam becomes bi-directional. High-resolution data (not presented here) show that the width of the beam on spacecraft 1, 3, and 2 was roughly the same as the width of the potential structure. The false colour code represents the number flux of electrons in counts per second ranging from 10^3 (dark blue) to 5×10^5 (red).

four spacecraft moved along essentially the same orbit separated by 100 s (Fig. 2). During this auroral crossing spacecraft 1, 3 and 2 observed a diverging, bipolar electric field (Fig. 3) changing from a southward to a northward direction. Together with a dominant east–west magnetic-field variation this implies that the structure was sheet-like and extended in the east–west direction. It grew in latitudinal width and magnitude, corresponding to an increase in the positive electric potential peak of the structure from 0.4 kV on Rumba, to 1.7 kV on Samba, to over 2 kV on Salsa. Accompanying this structure was an upward uni-directional electron beam, increasing in energy (from about 0.7 keV on Rumba, to 1.2 keV on Samba, and to 2.0 kV on Salsa), as well as in width (Fig. 4). However, when Tango reached the position of the structure, the electric field structure and the unidirectional upward electron beam had vanished. The electric field structure and associated upward electron beam are located in the transition region between the central plasma sheet and the plasma sheet boundary layer. The region of diffuse aurora seen in the post-midnight auroral oval (Fig. 2) corresponds to the central plasma sheet electron precipitation, whereas the darker region just poleward of it corresponds to the plasma sheet boundary layer. This transition is also indicated by the gradient in the plasma density, which first steepens as the electric field increases, then becomes less steep as the electric field structure widens, and finally fades away together with the electric field at the time of the last crossing. The field-aligned current associated with the structure is downward, as shown in Fig. 3b. The total downward current integrated over the structure remains roughly constant during the crossings by the four spacecraft, whereas the width of the current sheet is seen to increase, in particular between the two last crossings.

The consistency between the evolution of the parallel acceleration potential (inferred from the energy of the upward electron beam) and that of the perpendicular potential (integrated from the electric field) indicates that the Cluster spacecraft were crossing the upper reaches of a U-shaped positive potential structure. The data show that this positive potential structure (diverging electric field structure) in the downward current region extends to altitudes greater than 20,000 km and that it grows in size and intensifies over a time period of a few hundred seconds, after which it fades away accompanied by a drop in the characteristic energy of the electron beam, a significant widening of the downward current sheet, and no distinct plasma density gradient. It has been shown by numerical simulations that this time period is comparable to the time it takes to evacuate the ionosphere electrons over the region of the downward current sheet[22]. This evacuation, accomplished by upward-moving electrons and by transport of ions perpendicular to the geomagnetic field in the lower ionosphere, implies an increasing load over the downward-field-aligned current branch of the auroral current circuit. From Freja observations[9] we know that both the occurrence and the magnitude of the diverging electric fields peak for minimum ionospheric conductivity conditions, near winter solstice and local midnight[9]. Thus, it is possible that the evolution of the potential structure, with its region of a parallel electric field predominantly above the ionosphere, is closely related to the formation of such ionospheric plasma density holes, although the nature of this relationship remains to be understood. Temerin and Carlson[16] have presented a model of the current–voltage relationship in the return current region based on quasi-neutrality. This model, however, does not include the plasma evacuation, which we believe is an essential feature of this region. A possible explanation for the fading of the potential structure by the time Tango reached its location may be found in the sudden widening of the return current sheet seen at this time (Fig. 3b). The current carriers now become available from a much wider region, so that the current can easily be maintained. This again agrees with the results from the numerical simulation of the return current dynamics that as the plasma density hole develops, charge carriers are collected from regions further and further away from the core of the return current flux tube.

The negatively charged auroral potential structure and the positively charged return current structure are connected to each other in a common current circuit (Fig. 1), driven by an external generator[23,24]. This generator may be connected with the diverging bipolar-electric-field structure observed, which could reflect a strong velocity shear, imposed by the magnetosphere at the interface between the central plasma sheet and the boundary plasma sheet. Whether the generator is connected along the magnetic field to the structure or not, the evolving potential structure and the associated ionospheric density hole form a growing load which influences the whole circuit, either through a direct feedback or through load redistribution, and thus it may have an impact on the ordinary visible aurora. □

Received 14 November; accepted 19 November 2001.

1. Reiff, P. H. *et al.* Determination of auroral electrostatic potentials using high- and low-altitude particle distributions. *J. Geophys. Res.* **93,** 7441–7465 (1988).
2. Block, L. P. & Fälthammar, C.-G. The role of magnetic field-aligned electric fields in auroral acceleration. *J. Geophys. Res.* **95,** 5877–5888 (1990).
3. McFadden, J. P., Carlson, C. W. & Ergun, R. E. Microstructure of the auroral acceleration region as observed by FAST. *J. Geophys. Res.* **104,** 14453–14480 (1999).
4. Chiu, Y. T., Newman, L. & Cornwall, J. M. On the structures and mapping of auroral electrostatic potentials. *J. Geophys. Res.* **86,** 10029–10037 (1981).
5. Klumpar, D. M. & Keikkila, W. J. Electrons in the ionospheric source cone: Evidence for runaway electrons as carriers for downward Birkeland currents. *Geophys. Res. Lett.* **9,** 873–876 (1982).
6. Gorney, D. J., Chiu, Y. T. & Croley, D. R. Jr Trapping of ion conics by downward parallel electric fields. *J. Geophys. Res.* **90,** 4205–4210 (1985).
7. Marklund, G. T., Blomberg, L. G., Fälthammar, C.-G. & Lindqvist, P.-A. On intense shock-like electric fields associated with black aurora. *Geophys. Res. Lett.* **21,** 1859–1862 (1994).
8. Marklund, G. T., Blomberg, L. G., Fälthammar, C.-G., Lindqvist, P.-A. & Eliasson, L. On the occurrence and characteristics of intense low-altitude electric fields observed by Freja. *Ann. Geophys.* **13,** 704–712 (1995).
9. Marklund, G., Karlsson, T. & Clemmons, J. On low-altitude particle acceleration and intense electric fields and their relationship to black aurora. *J. Geophys. Res.* **102,** 17509–17522 (1997).
10. Carlson, C. W. *et al.* FAST observations in the downward auroral current region: energetic upgoing electron beams, parallel potential drops, and ion heating. *Geophys. Res. Lett.* **25,** 2017–2020 (1998).
11. Ergun, R. E. *et al.* FAST satellite observations of electric field structures in the auroral zone. *Geophys. Res. Lett.* **25,** 2025–2028 (1998).
12. Alfvén, H. On the theory of magnetic storms and aurorae. *Tellus* **10,** 104–116 (1958).
13. Borovsky, J. E. Auroral arc thicknesses as predicted by various theories. *J. Geophys. Res.* **98,** 6101–6138 (1993).
14. Carlqvist, P. & Boström, R. Space-charge regions above the aurora. *J. Geophys. Res.* **75,** 7140–7146 (1970).
15. Boström, R. Voltage drops along auroral magnetic field lines on small and large scale. *Phys. Space Plasmas* **15,** 37–42 (1998).
16. Temerin, M. & Carlson, C. W. Current–voltage relationship in the downward auroral current region. *Geophys. Res. Lett.* **25,** 2365–2368 (1998).
17. Rönnmark, K. Electron acceleration in the auroral current circuit. *Geophys. Res. Lett.* **26,** 983–986 (1999).
18. Wygant, J. R. *et al.* Polar spacecraft based comparisons of intense electric fields and Poynting flux near and within the plasma sheet tail lobe boundary to UVI images: An energy source for the aurora. *J. Geophys. Res.* **105,** 18675–18692 (2000).
19. Keiling, A. *et al.* Properties of large electric fields in the plasma sheet at 4-7 R_E measured with Polar. *J. Geophys. Res.* **106,** 5779–5798 (2001).
20. Escoubet, C. P., Russel, C. T. & Schmidt, R. (eds) The Cluster and Phonix Missions. *Space Sci. Rev.* **79** (1/2), 1–658 (1997).
21. Issue on Cluster first results. *Ann. Geophys.* **19** (October/November 2001).
22. Karlsson, T. & Marklund, G. Simulations of effects of small-scale auroral current closure in the return current region. *Phys. Space Plasmas* **15,** 401–406 (1998).
23. Vasyliunas, V. M. in *Particles and Fields in the Magnetosphere* (ed. McCormac, B.) 60–71 (Reidel, Dordrecht, 1969).
24. Lysak, R. L. Electrodynamic coupling of the magnetosphere and ionosphere. *Space Sci. Rev.* **52,** 33–87 (1990).

Acknowledgements

We are indebted to H. Frey for providing the IMAGE data for the event, and G. Gustavsson who was the Principal Investigator for the Electric Field and Wave (EFW) instrument until 2000.

Competing interests statement

The authors declare that they have no competing financial interests.

Correspondence and requests for materials should be addressed to G.T.M. (e-mail: marklund@plasma.kth.se).